

Combined Effect of Temperature and Humidity on Distorted Currents Measured by Rogowski Coils

Federica Costa, Alessandro Mingotti, Lorenzo Peretto, and Roberto Tinarelli

Department of Electric, Electronic and Information Engineering

University of Bologna

Bologna, Italy

federica.costa13, alessandro.mingotti2, lorenzo.peretto, roberto.tinarelli3@unibo.it

Abstract—The necessity of accelerating towards carbon neutrality has been further pushed in recent times. Therefore, with the aim of developing smart grids, new Intelligent Electronic Devices (IEDs) are being widely installed. In this regard, Low Power Current Transformers (LPCTs) are replacing traditional inductive current transformers (CTs). Among these, Rogowski coils feature high linearity, reduced dimensions, and wide bandwidth in comparison to CTs. Hence, this work presents a study on a particular type of LPCT, the Rogowski coil, which is extensively used nowadays. In detail, temperature and humidity are simultaneously applied to three commercial Rogowski coils when measuring off-nominal, hence distorted, currents. The LPCTs performances are evaluated in terms of power quality indexes, Total Harmonic Distortion (THD) and single harmonic evaluation. From the results, THD is not significantly affected by the combined temperature/humidity presence. However, a deep analysis on the single harmonic demonstrated how they are strongly correlated to such influence quantities. It is interesting to highlight that each of the three devices under test present different behaviors. It is then crucial to in deep the investigation on the influence quantities affecting LPCTs. Furthermore, International Standards should include new details and test procedures to assess the effect on the LPCTs accuracy due to such quantities.

Keywords— *Low power instrument transformer, Rogowski coil, LPCT, distorted signals, power quality, temperature, humidity, influence quantities.*

I. INTRODUCTION

In the recent years, there has been an urge to accelerate the decarbonization of the EU energy system, which aims at reaching carbon neutrality by 2050 [1-3].

In order to do so, the spread of Renewable Energy Sources (RESs) in power systems, especially wind and solar, has been further pushed [4,5].

Despite their positive contribution to the carbon neutrality, RESs are impacting on the harmonic pollution level of the grid. Such a level can be assessed, in terms of voltage and frequency characteristics, by referring to the international Standard EN 50160 [6]. It provides ranges within which the electrical quantities should remain during normal and faulty conditions.

Many other assets have been developed and have been increasingly installed in power systems to achieve the so-called smart grids. It is worth recalling smart meters and Intelligent Electronic Devices (IEDs) [7,8]. In addition, traditional inductive instrument transformers (ITs) are being progressively replaced by Low Power Instrument Transformers (LPITs).

Specifically, among all existing LPITs, this work focuses on Rogowski coils. They feature reduced dimensions implying easiness in their installation, wider bandwidths, and lighter weights in comparison to inductive ITs.

Hence, the aim of this work is to assess the accuracy performance of Rogowski coils when measuring currents with different levels of distortion. Furthermore, such measurements are performed under the simultaneous presence of temperature and humidity variations.

Looking at the literature, some slightly relevant works can be found. For instance, [9] deals with the evaluation of distorted signals by Rogowski coils and [10] studies new solutions to extend the bandwidth of these devices. Nevertheless, in [9] neither the effects of temperature nor those of humidity are addressed.

In [11-13] authors only discuss the effect of positioning on the performances of Rogowski coils, whereas [14] treats multiple influence quantities, such as positioning, frequency, and temperature. However, among these, neither power quality nor humidity are studied.

The authors in [15] analyzed how the temperature affects Rogowski coils, based on a thermoelastic theory. Yet, the effects of humidity are not considered in this study.

Other studies, instead, focus on the modelling of such devices, as done by the authors in [16-18].

As for the sections of IEC 61869 Standard dedicated to general aspects of ITs and LPITs, documents 61869-1 and 61869-6 [19,20], respectively, they do not provide neither information about humidity nor how to perform tests. Hence, to the best of authors' knowledge, this study introduces novelties to the current literature.

Therefore, the added value of this work is the analysis on how the combined effect of temperature and humidity affects the accuracy performances of Rogowski coils. In particular, when they are measuring distorted currents.

The remainder of the paper is organized as follows: Section II presents the theoretical and normative background relevant to Rogowski coils and Low Power Current Transformers (LPCTs). Section III illustrates the adopted measurements setup and the specifications of its main components. Section IV shows the experimental tests, whereas in Section V the main results. Finally, Section VI draws some conclusions and presents future developments.

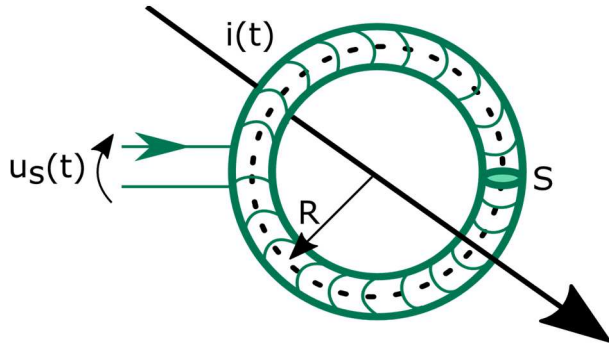


Figure 1. Structure of a Rogowski coil.

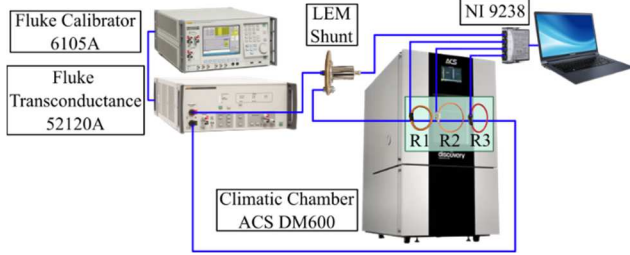


Figure 2. Adopted measurement setup.

TABLE I. MAIN SPECIFICATIONS OF THE MEASUREMENT SETUP

Device	Specifications	
Fluke 6105A and Fluke 52120A	up to 850 Hz	0.009 % and 0.002 % (percentage of output and range)
	up to 6 kHz	0.040 % and 0.004 %
LEM shunt	100 A/1 mΩ	
ACS DM600	Temp. range: 10 to 95 °C (for humidity tests) Temp. fluctuations: ± 0.1 to ± 0.3 K Temp. changing rate: 4.5 K/min Humidity range: 10 to 98 % Humidity fluctuations: ± 1 to ± 3 %	
NI 9238	ADC: 24-bit Max sampling rate: 50000 Sa/s/ch Input impedance: >1 GΩ Voltage range: ± 500 mV	

TABLE II. ROGOWSKI COILS UNDER TEST CHARACTERISTICS

Info	Rogowski coil		
	R1	R2	R3
Voltage output (mV/kA)	100	100	100
Frequency range (Hz)	20 – 5k	1 – 50k	50 – 60
Accuracy (%)	± 1	± 0.5	± 1
Temperature range (°C)	-20 to +70	-40 to +80	-20 to +80

II. THEORETICAL AND NORMATIVE BACKGROUND

A. Rogowski Coils Working Principle

Rogowski coils are a particular type of LPITs which is widely used to perform current measurements. Their typical schematic is presented in Fig. 1.

The operating principle of a Rogowski is based on Ampere's law. It relates the magnetic field H around a closed loop l to the current i passing through the loop, as:

$$\oint_0^l \vec{H} \cdot d\vec{l} = i. \quad (1)$$

It is then straightforward to obtain the equation that rule the Rogowski coil working principle:

$$u_s(t) = -M \frac{di(t)}{dt}, \quad (2)$$

where u_s is the measured voltage related to the unknown current i via the mutual induction coefficient M , which comprises also geometrical factors such as the cross-section S and the radius R .

B. Normative Background

According to [19], ITs are classified into three main categories depending on their minimum and maximum ambient temperatures.

In all categories, the maximum temperature is set at 40 °C, whereas the minimum one can be -5, -25, or -40 °C. This results in -5/40, -25/40, and -40/40 categories.

Furthermore, the same Standard [19] provides information about the steady-state temperatures in ITs. A steady-state temperature is reached when the rate of temperature rise does not exceed 1 K/h.

Nevertheless, as far as humidity is concerned, neither [21] nor [22], respectively dedicated to LPCTs and Low Power Voltage Transformers (LPVTs), provide any information about which tests should be carried out, nor how ratio error and phase displacement may change.

III. MEASUREMENT SETUP

The developed setup is illustrated in Fig. 2.

The calibrator is used jointly with the transconductance to generate two sets of distorted currents. These are then measured by a resistive shunt and the Rogowski Under Test (RUTs) located inside the climatic chamber. It is worth highlighting that the current-carrying conductor is perfectly aligned with the vertical and horizontal symmetry axes of the RUTs.

The RUTs and the shunt output voltages are acquired by a DAQ board, NI 9238, which is controlled using LabVIEW. For each test, a waveform is acquired every 10 minutes, ensuring that enough measurements are considered for each temperature plateau and ramp.

Table I presents the main characteristics of the utilized devices, whereas Table II the specification of the RUTs.

More information about the measurement setup and RUTs can be found in [9].

IV. EXPERIMENTAL TESTS

A combined temperature and humidity cycle has been used to tests the Rogowski coils. In section A the cycle is described. Afterwards, sections B and C introduce the adopted signals and the parameters used for their evaluation, respectively.

A. Temperature and Humidity

The temperature cycle has been defined according to [20]. In addition, a humidity cycle has been superimposed to it. The obtained combined cycle can be seen in Fig. 3. The cycle starts with a relative humidity of 30 %. Once the room temperature of + 23 °C is reached, then it is hold constant for

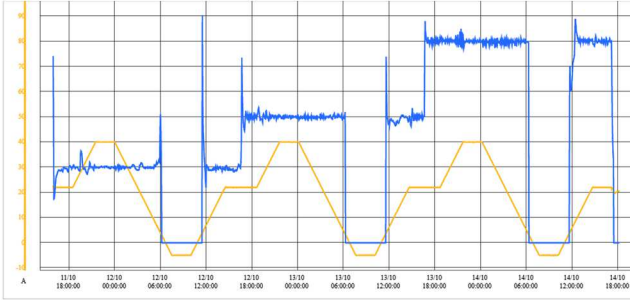


Figure 3. Temperature and humidity cycles performed in the climatic chamber.

2 hours and 30 minutes. Afterwards, the next setpoint of 40 °C is reached at a slope of 0.1 °C/min in 3 hours, which is followed by a plateau of the same time length, i.e., 2 hours and 30 minutes. Finally, the last setpoint of -5°C is reached at the same slope as before, but in 7 hours and 30 minutes.

After keeping this temperature constant for 2 hours and 30 minutes, the cycle can start again fixing the next humidity setpoint which is 50 % and, lastly, 80 %.

In Fig. 3, the yellow trace represents the temperature, whereas the blue one the humidity. The y-axis is common for both temperature (°C) and humidity (%).

Note that the intervals between temperature and humidity values have been designed according to the Standards and to the device characteristics. The missing information is then replaced with authors' gained experience.

B. Distorted Currents

To evaluate the performances of the RUTs, two different distorted currents have been applied.

In order to create appropriate sets of data, EN 50160 [6] and IEEE Standard 519 [23] have been considered. The first one provides the most common harmonics in power systems, whereas the last one the THD maximum levels.

In what follows, two distorted signals are referred to as H1 and H2. Test H1 has a THD of 4.8 % obtained with a mix of harmonics from the 3rd to the 35th. While test H2 features a THD of 9.2 % achieved with harmonics from the 3rd to the 41st. It is worth underlying that these harmonics are going to be superimposed to a 50 Hz sinusoidal current having an amplitude of 80 A rms.

C. Parameters to be Evaluated

During the combined temperature and humidity cycle, each set of measurements has been manipulated as follows. In LabVIEW, a DFT analysis is performed over 10000 samples acquired at the maximum sampling rate available with the used DAQ (50000 Sa/s/ch), corresponding to an observation window of 200 ms for a 50 Hz signal.

A waveform is acquired every 10 minutes, resulting in a total of 438 assessments per each test H1 and H2.

The following quantities are then computed:

1) *THD*: from the acquired waveforms, both the 50 Hz component and the superimposed harmonics are extracted to compute the THD expressed as:

$$THD = \frac{\sqrt{\sum_{h=2}^N I_{h,RMS}^2}}{I_{1,RMS}} \times 100, \quad (3)$$

where $I_{1,RMS}$ is the RMS value of the 50 Hz component and $I_{h,RMS}$ are the RMS values of the h harmonics.

Moreover, given that the objective of this work is to assess the combined effect of temperature and humidity on RUTs when measuring distorted currents, an additional quantity providing detailed information about the trend of the THD during the cycle is evaluated.

In detail, the first THD measurement, THD (1), is considered as a reference value for all the others, therefore the difference between the latter and all the other 437 measurements, THD (n) where $n = 2, 3, \dots, 437$, is performed during the temperature and humidity cycle, resulting in ΔTHD as:

$$\Delta THD = THD (1) - THD (n). \quad (4)$$

2) *Harmonic currents*: the harmonic currents, already extracted to perform the previous computation of the THD, are evaluated.

Specifically, the smallest and the biggest superimposed harmonic are assessed. For this reason, in test H1, the 3rd and the 35th harmonic are calculated; whereas for test H2, the 3rd and the 41st. Following the same rationale illustrated before, the difference between the first measured harmonic $I_h (1)$ and all the other measured harmonics $I_h (n)$, where $n = 2, 3, \dots, 437$ is computed as $\Delta I_h (A)$ and it is shown in (5):

$$\Delta I_h = I_h (1) - I_h (n), \quad (5)$$

where $h = 3, 35, 41$ represents the harmonic order.

V. TEST RESULTS

This Section aims at presenting the most significant results obtained from the tests detailed in the previous Section IV.

The variations of the extracted quantities with respect to their corresponding first measurement, ΔTHD and ΔI_h , are analyzed.

1) *THD*: From top to bottom, the three plots of Fig. 4 present the results obtained from RUT R1, R2 and R3, respectively. Blue dots represent ΔTHD measured in case of H1 testing condition, whereas the green ones show H2.

As shown in Fig. 4, for R1, the results of H1 and H2 are comparable since there are no major fluctuations in neither case: the outcomes oscillate around 0 % with some spikes up to ± 0.20 %.

On the other hand, results from R2 and R3 differ from the previous ones, even if they provide a similar behavior.

The fluctuations noticeable in test H1 are clearly smaller than those from test H2 and, additionally, the spikes measured in H2 correspond for both R2 and R3.

Note however, that from H1 and H2 results it is noticeable that H1 causes a negative bias (hence a higher ΔTHD). The opposite can be observed for H2. What is interesting is that both behaviors are recorded for all tested Rogowski coils.

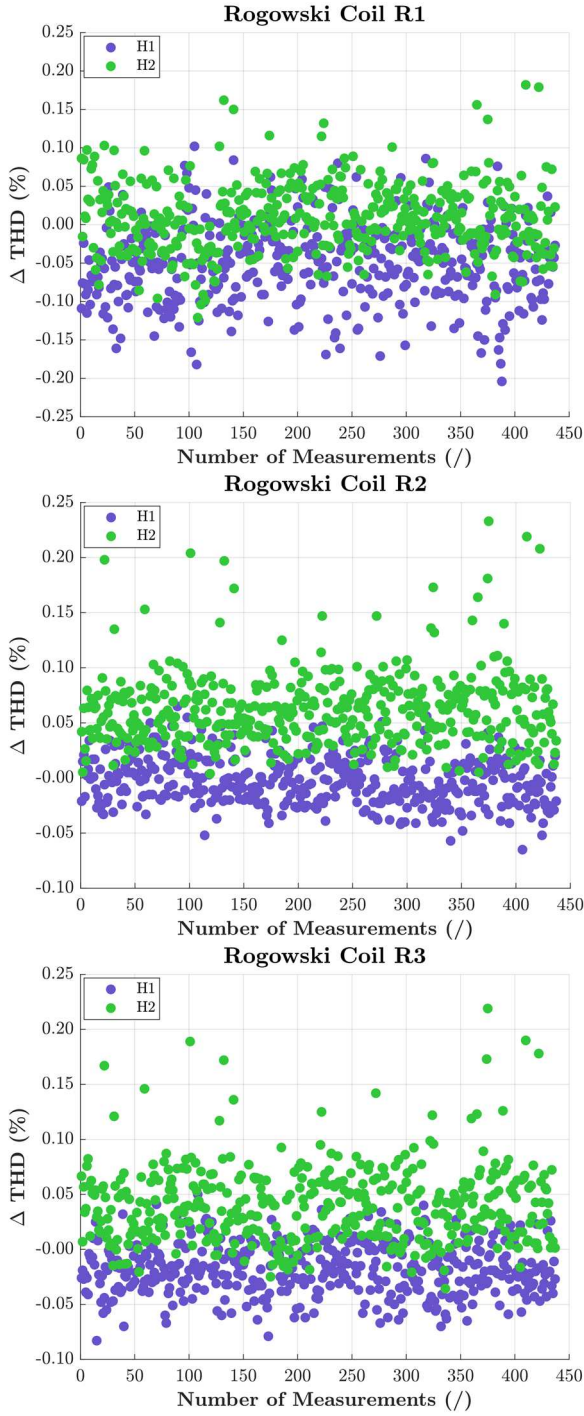


Figure 4. THD variation ($\Delta\text{THD} (\%)$) results for the RUTs.

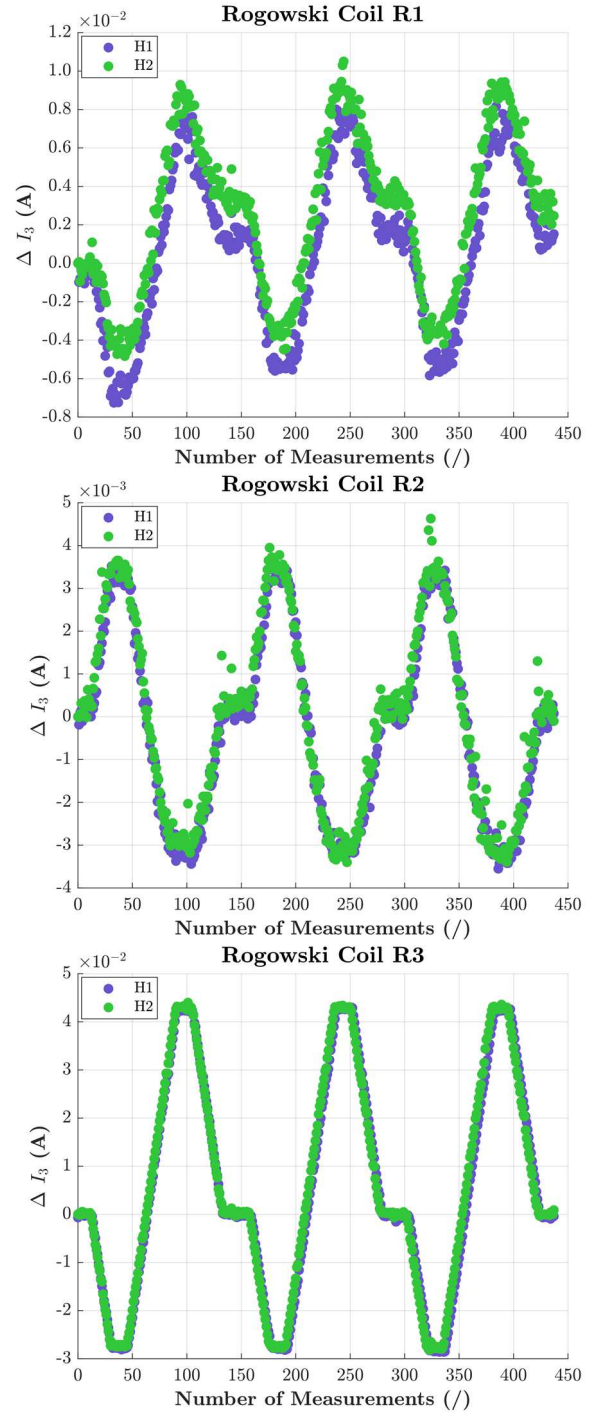


Figure 5. Variation of the 3rd harmonic current for the RUTs.

2) *Harmonic currents*: in Fig. 5, the 3rd harmonic for both tests H1 and H2 is plotted. This has been done in order to assess whether the intensity of harmonic content implies a worsening in the estimation of the harmonics, since no specific correlation can be retrieved from the previous THD results. In this case, three different behaviors can be noted, one per each RUT.

For R1, the 3rd harmonic varies from roughly -0.008 A to 0.010 A. The trend of the harmonic current resembles the temperature and humidity cycle, even though vertically

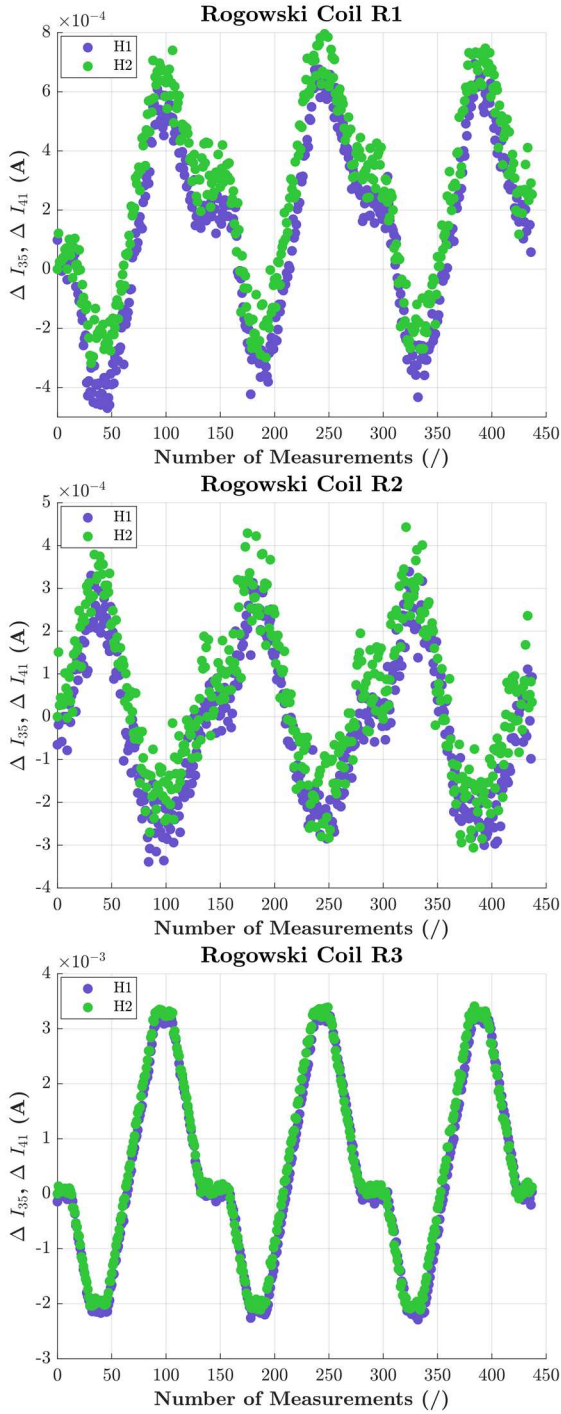


Figure 6. Variation of the 35th and 41st harmonic currents for the RUTs.

mirrored. Some discrepancies can be identified between tests H1 and H2, but not significant.

For R2, the same comment on the harmonic behavior applies. In this case, though, the fluctuations are reduced as the extremes range from -3.5 to 4 mA. Moreover, the differences between H1 and H2 are negligible.

For R3, instead, different observations arise. Its pattern is mirrored as for R1, but in this case the edges are sharper and discrepancies between H1 and H2 are negligible. No spikes outside the general trend of the plot are present. Finally, it is worth noting that this case is the one showing the highest fluctuations, ranging from -0.030 to 0.045 A.

Turning to the highest harmonic component (the 35th for H1 and the 41st for H2), the graphs for the three RUTs are

collected in Fig. 6. Note that, despite the different harmonic order, the same amplitude is set as a percentage of the RMS of the 50 Hz component, therefore the same results are expected.

At a glance, all three RUTs are characterized by trends similar to those observed in Fig. 5, albeit smaller fluctuations can be noted. Nevertheless, for R1 and R2 the cycle pattern is more undefined and higher spikes are measured in proximity to the lowest and highest peaks.

Contrarily, for R3, the pattern is still sharp, and no spikes are recorded also in this case.

Having analyzed the outcomes, it can be concluded that THD is not significantly affected by the combination of temperature and humidity. Despite this, some spikes could be noted in correspondence to the highest temperature (40 °C). Considering that THD is an index that includes many information and quantities, the smallest and the biggest harmonic components have been evaluated.

It resulted that the harmonics behavior follows the temperature/humidity cycle.

An interesting feature which could be mentioned is that, even though the same currents were injected, the three RUTs presented very different oscillations and ranges of variation, nonetheless positive/negative spikes were the same. Therefore, it can be concluded that, even if from THD the effect of the cycle is not noticeable, it is when single harmonics are considered.

VI. CONCLUSIONS

This paper presented a study concerning the combined effect of temperature and humidity on the evaluation of distorted currents by Rogowski coils.

This study was conducted considering that Standards do not provide any specific information about how to perform these combined tests and whether ratio error and phase displacement change in presence of such influence quantities.

The results have shown that the temperature plays a significant role in the measured harmonics, but in distinct ways for each of the three RUTs. Furthermore, harmonics, singularly addressed, show a strict relation with humidity and temperature variations.

Future developments will be devoted to a further analysis of the combined of other influence quantities.

REFERENCES

- [1] S. Potrč, L. Čuček, M. Martin, and Z. Kravanja, "Sustainable renewable energy supply networks optimization – The gradual transition to a renewable energy system within the European Union by 2050," *Renew. Sustain. Energy Rev.*, vol. 146, 2021, doi: 10.1016/j.rser.2021.111186.
- [2] M. Andrei, P. Thollander, I. Pierre, B. Gindroz, and P. Rohdin, "Decarbonization of industry: Guidelines towards a harmonized energy efficiency policy program impact evaluation methodology," *Energy Reports*, vol. 7, pp. 1385–1395, 2021, doi: 10.1016/j.egy.2021.02.067.
- [3] D. Amaripadath *et al.*, "Power quality disturbances on smart grids: Overview and grid measurement configurations," in *2017 52nd International Universities Power Engineering Conference, UPEC 2017*, 2017, vol. 2017-Janua, pp. 1–6, doi: 10.1109/UPEC.2017.8231975.
- [4] S. G. Simoes *et al.*, "Climate proofing the renewable electricity deployment in Europe - Introducing climate variability in large energy systems models," *Energy Strateg. Rev.*, vol. 35, 2021, doi: 10.1016/j.esr.2021.100657.
- [5] A. Chehri, R. Saadane, I. Fofana, and G. Jeon, *Smart Grid for Sustainable Cities: Strategies and Pathways for Energy Efficiency Solutions*, vol. 263. 2022.

- [6] H. Markiewicz, A. Klajn, and W. University of Technology, "Standard EN 50160 Voltage Characteristics in Public Distribution Systems 5.4.2," 2004. [Online]. Available: www.lpqi.org.
- [7] E. C. Piescirovsky, T. Smith, S. K. Mukherjee, and M. W. Marshall, "A generic method for interfacing IEDs using low voltage interfaces to real-time simulators with hardware in the loop," *Electr. Power Syst. Res.*, vol. 199, 2021, doi: 10.1016/j.epsr.2021.107431.
- [8] V. G. Vilas, V. Muralidhara, S. M. Bakre, and V. Velhal, "Smart meter modelling and fault location communication in Smart Grid," *Majlesi J. Electr. Eng.*, vol. 12, no. 2, pp. 55–62, 2018.
- [9] A. Mingotti, F. Costa, R. Tinarelli, and L. Peretto, "External Magnetic Fields Effect on Harmonics Measurements with Rogowski coils," in *11th IEEE International Workshop on Applied Measurements for Power Systems, AMPS 2021*, 2021, p. 6.
- [10] W. Zhang, F. Wang, and B. Holzinger, "High-bandwidth shielded rogowski coil current sensor for SiC MOSFET power module," in *Conference Proceedings - IEEE Applied Power Electronics Conference and Exposition - APEC*, 2021, pp. 1242–1249, doi: 10.1109/APEC42165.2021.9487370.
- [11] M. Chiampi, G. Crotti, and A. Morando, "Evaluation of flexible rogowski coil performances in power frequency applications," *IEEE Trans. Instrum. Meas.*, vol. 60, no. 3, pp. 854–862, 2011, doi: 10.1109/TIM.2010.2060223.
- [12] L. Ferković, D. Ilić, and I. Leniček, "Influence of Axial Inclination of the Primary Conductor on Mutual Inductance of a Precise Rogowski Coil," *IEEE Trans. Instrum. Meas.*, vol. 64, no. 11, pp. 3045–3054, 2015, doi: 10.1109/TIM.2015.2444254.
- [13] L. Ferkovic, D. Ilic, and R. Malaric, "Mutual inductance of a precise Rogowski coil in dependence of the position of primary conductor," *IEEE Trans. Instrum. Meas.*, vol. 58, no. 1, pp. 122–128, 2009, doi: 10.1109/TIM.2008.928412.
- [14] Oganyan, R., M. Lankin, and N. Gorbatenko. 2020. "Research of the Effect of Displacement Primary Winding of a Measuring Current Transformer Based on the Rogowski Coil on the EMF of Secondary Winding." doi:10.1109/ICIEAM48468.2020.9111962
- [14] A. Mingotti, L. Peretto, and R. Tinarelli, "Effects of Multiple Influence Quantities on Rogowski-Coil-Type Current Transformers," *IEEE Trans. Instrum. Meas.*, vol. 69, no. 7, pp. 4827–4834, Jul. 2020, doi: 10.1109/TIM.2019.2953419.
- [15] P. Wang, F. Cheng, L. Ping, and Z. Shen, "Temperature characteristics of Rogowski coil current sensors," in *I2MTC 2018 - 2018 IEEE International Instrumentation and Measurement Technology Conference: Discovering New Horizons in Instrumentation and Measurement, Proceedings*, 2018, pp. 1–6, doi: 10.1109/I2MTC.2018.8409691.
- [16] Mingotti, A., L. Peretto, and R. Tinarelli. 2020. "A Smart Frequency Domain-Based Modeling Procedure of Rogowski Coil for Power Systems Applications" *IEEE Transactions on Instrumentation and Measurement* 69 (9): 6748–6755. doi:10.1109/TIM.2020.2986864.
- [17] Mingotti A, Peretto L, Tinarelli R. Smart Characterization of Rogowski Coils by Using a Synthesized Signal. *Sensors*. 2020; 20(12):3359. <https://doi.org/10.3390/s20123359>.
- [18] X. Liu, H. Huang and Y. Dai, "Effect of Frequency on the Linearity of Double-Layer and Single-Layer Rogowski Coils," in *IEEE Sensors Journal*, vol. 20, no. 17, pp. 9910–9918, 1 Sept.1, 2020, doi: 10.1109/JSEN.2020.2988073.
- [19] IEC 61869-1:2010, "Instrument transformers - Part 1: General requirements", International Standardization Organization, Geneva, Switzerland, 2010.
- [20] IEC 61869-6. Part 6: Additional general requirements for low-power instrument transformers. In *Instrument Transformers*; International Standardization Organization: Geneva, Switzerland, 2016.
- [21] IEC 61869-10. Part 10: Additional requirements for low-power passive current transformers. In *Instrument Transformers*; International Standardization Organization: Geneva, Switzerland, 2018.
- [22] IEC 61869-11:2018, "Instrument transformers - Part 11: Additional requirements for low-power passive voltage transformers", International Standardization Organization, Geneva, Switzerland, 2018.
- [23] IEEE Std 519-2014, "Recommended Practice and Requirements for Harmonic Control in Electric Power Systems", New York, USA, 2014.